$\rho_2 > \rho_1$: Lower curvature in medium 2, $\theta_2 < \theta_1$

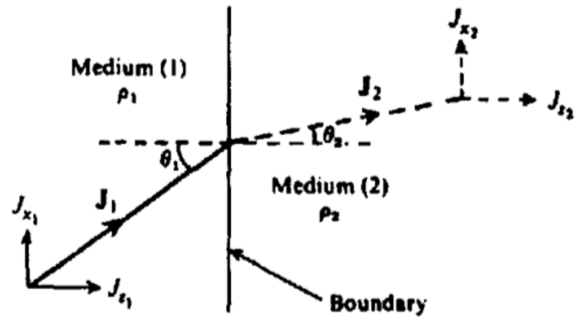

Figure 8.8. Distortion of current flow at a plane boundary when $\rho_1 < \rho_2$.

using Ohm's law to express these results in terms of the current density, we obtain

$$J_{x_1}\rho_1 = J_{x_2}\rho_2 \quad \text{and} \quad J_{z_1} = J_{z_2}$$

Dividing these expressions, we have

$$\rho_1(J_{x_1}/J_{z_1}) = \rho_2(J_{x_2}/J_{z_2}) \quad \text{or} \quad \rho_1 \tan\theta_1 = \rho_2 \tan\theta_2$$

so that

$$\tan\theta_2/\tan\theta_1 = \rho_1/\rho_2 \qquad (8.16)$$

Thus the current lines are bent in crossing the boundary. If $\rho_1 < \rho_2$, they will be bent toward the normal and vice versa.

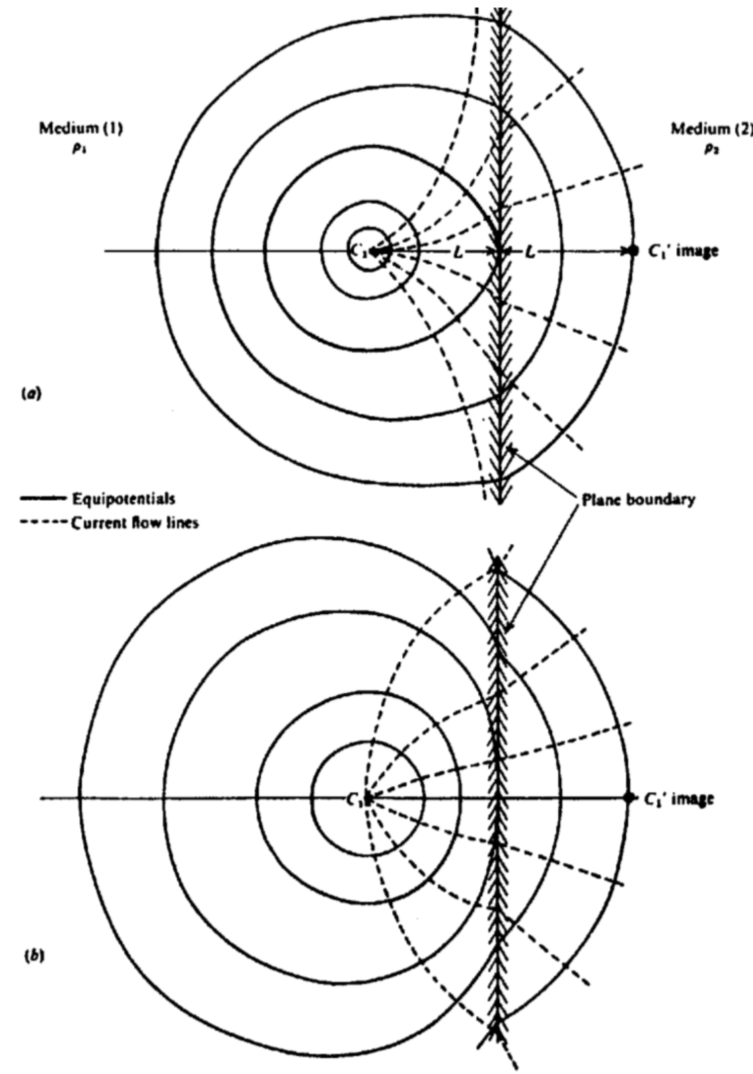

$\rho_2 < \rho_1$: Higher curvature in medium 2, $\theta_2 > \theta_1$

NOTE: ***Opposite*** to effect of velocity in Snell's Law of refraction – and ***Tangent***, not ***Sine*** of "incident" angle, $\boldsymbol{\theta}$!!!

Profiling maintains constant a-spacing while moving the array laterally. Wenner array ρ_{app} for a vertical contact:

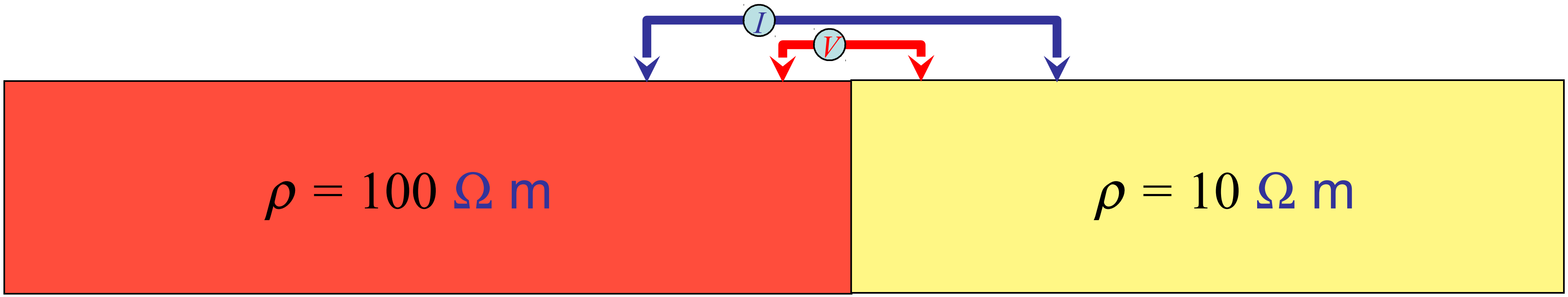

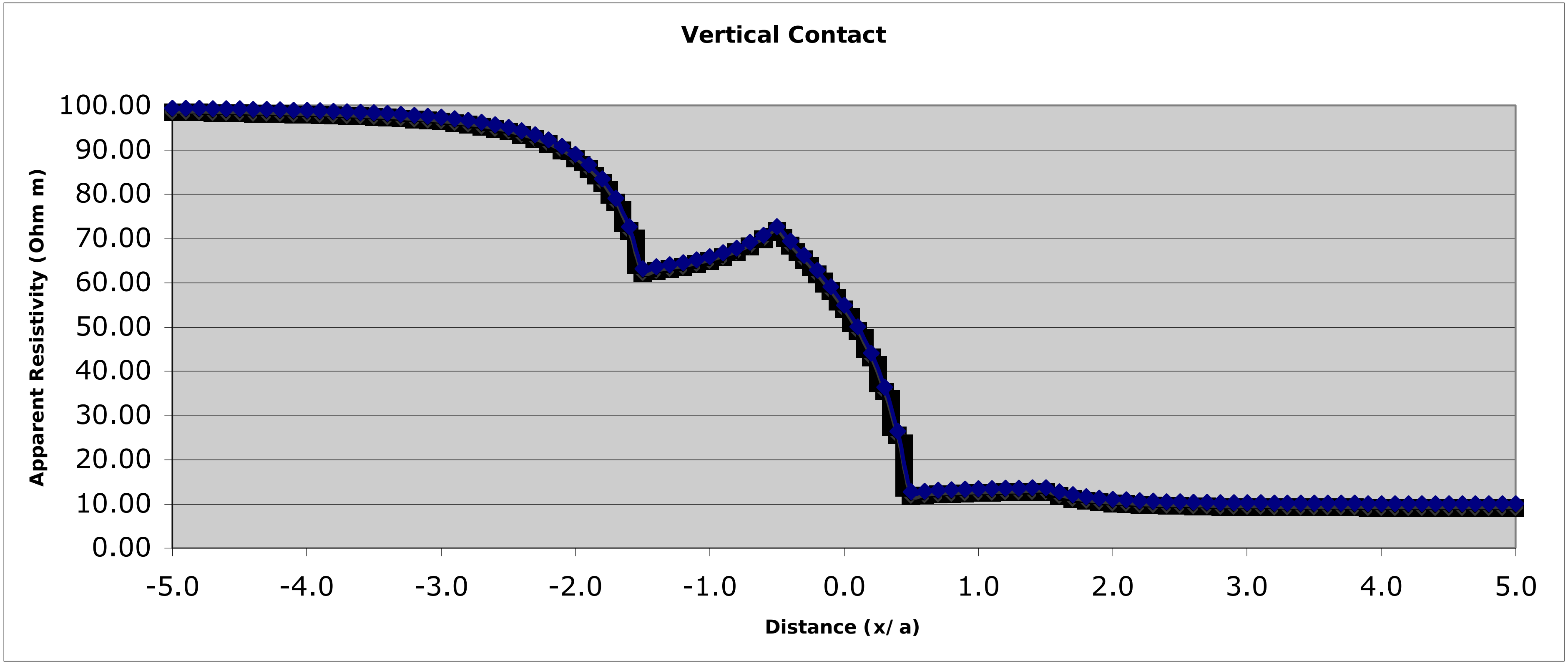

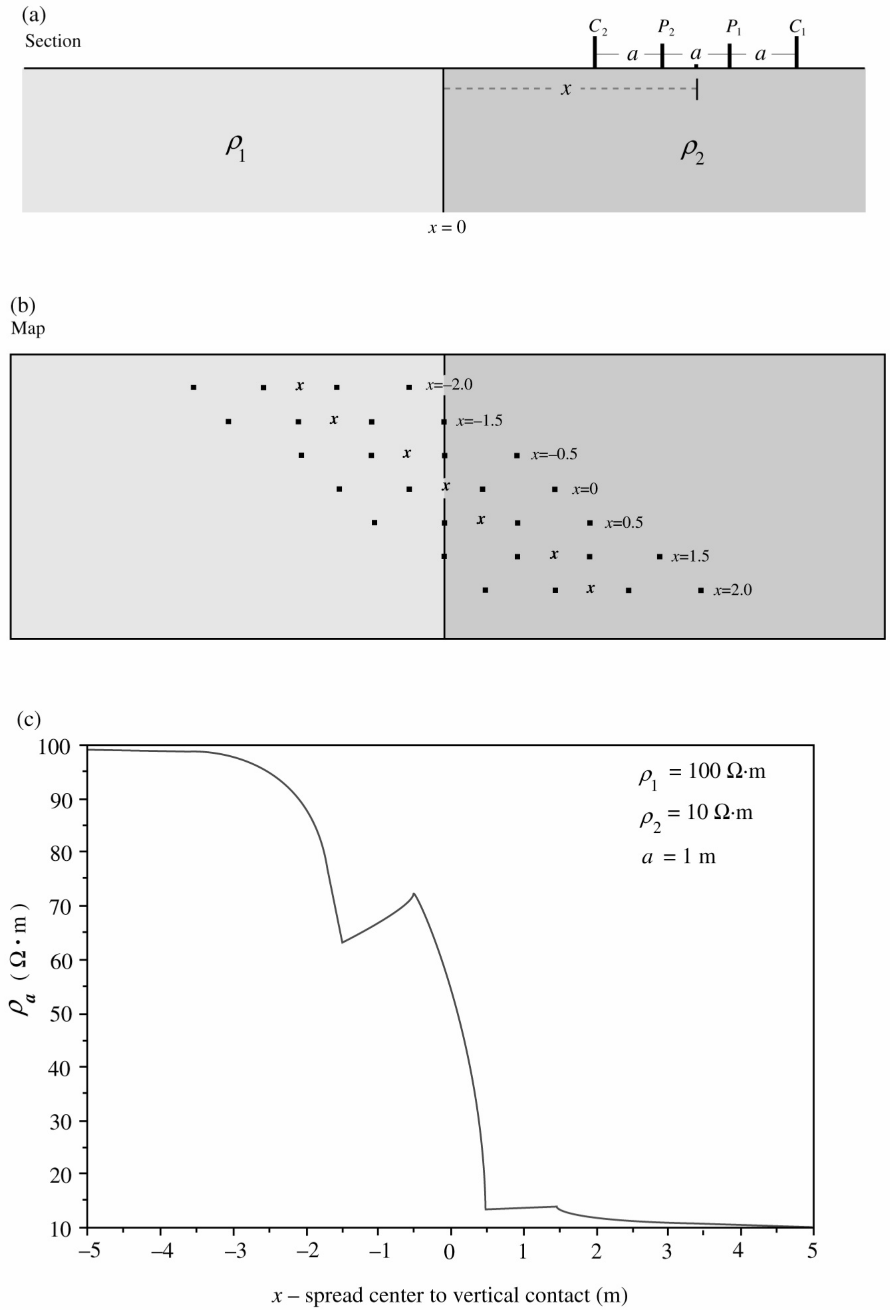

FIGURE 5.23g (c)

Sounding maintains a constant center while increasing the a-spacing. Wenner array ρ_{app} for a vertical contact:

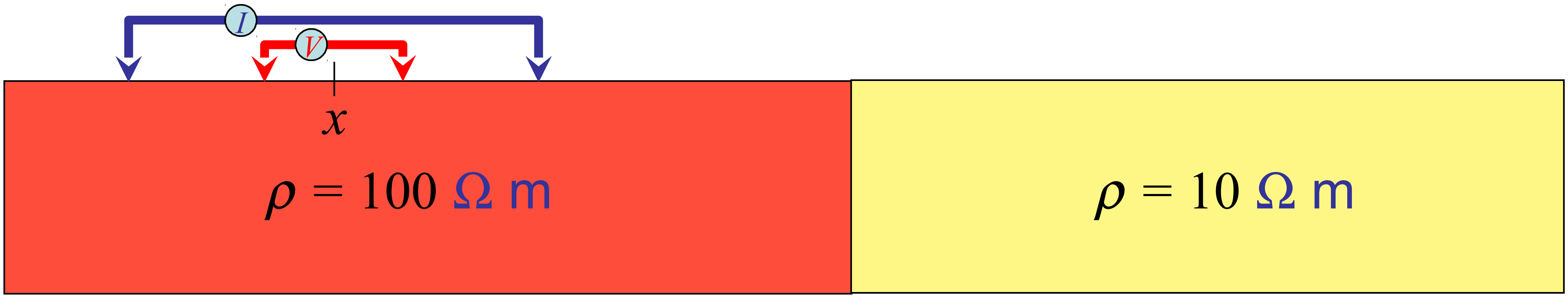

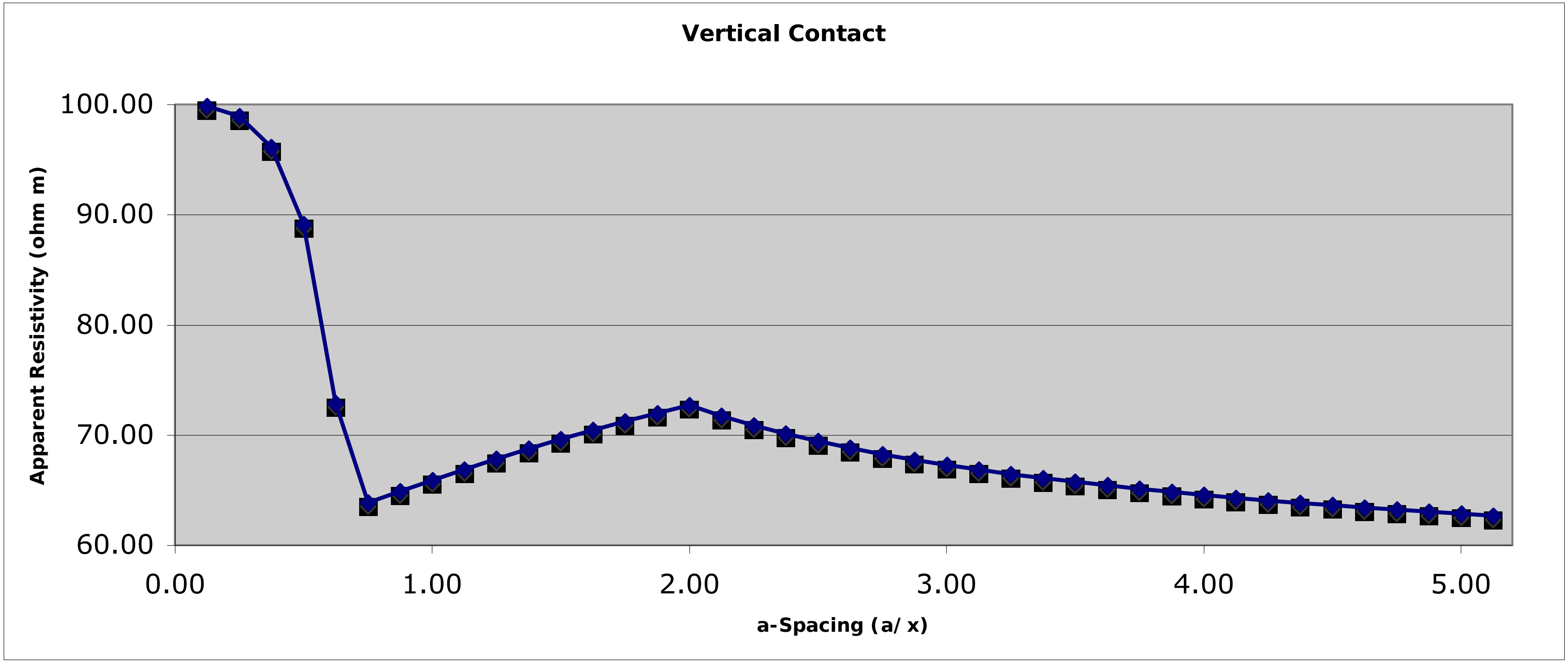

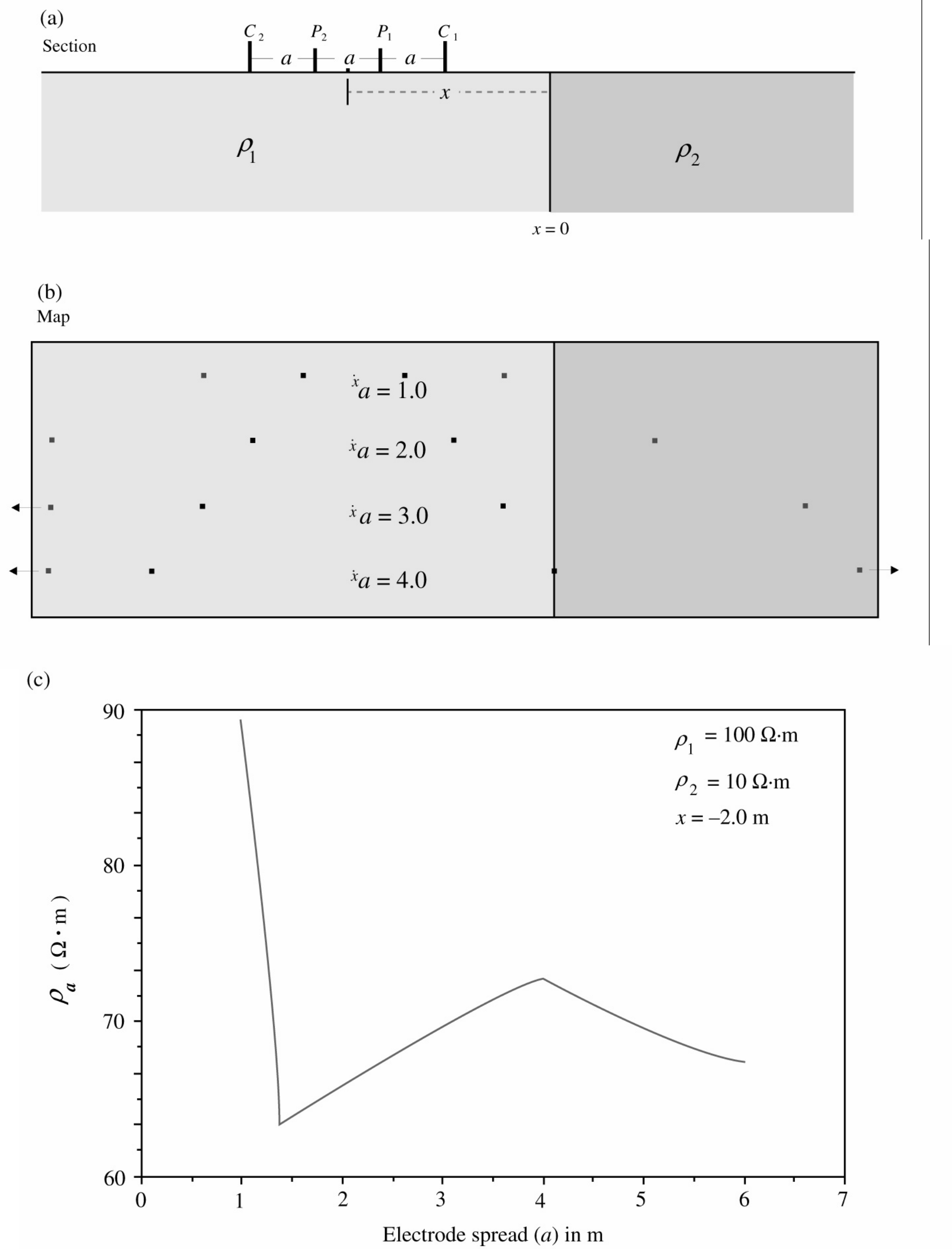

FIGURE 5.24g (c)

Introduction to Applied Geophysics

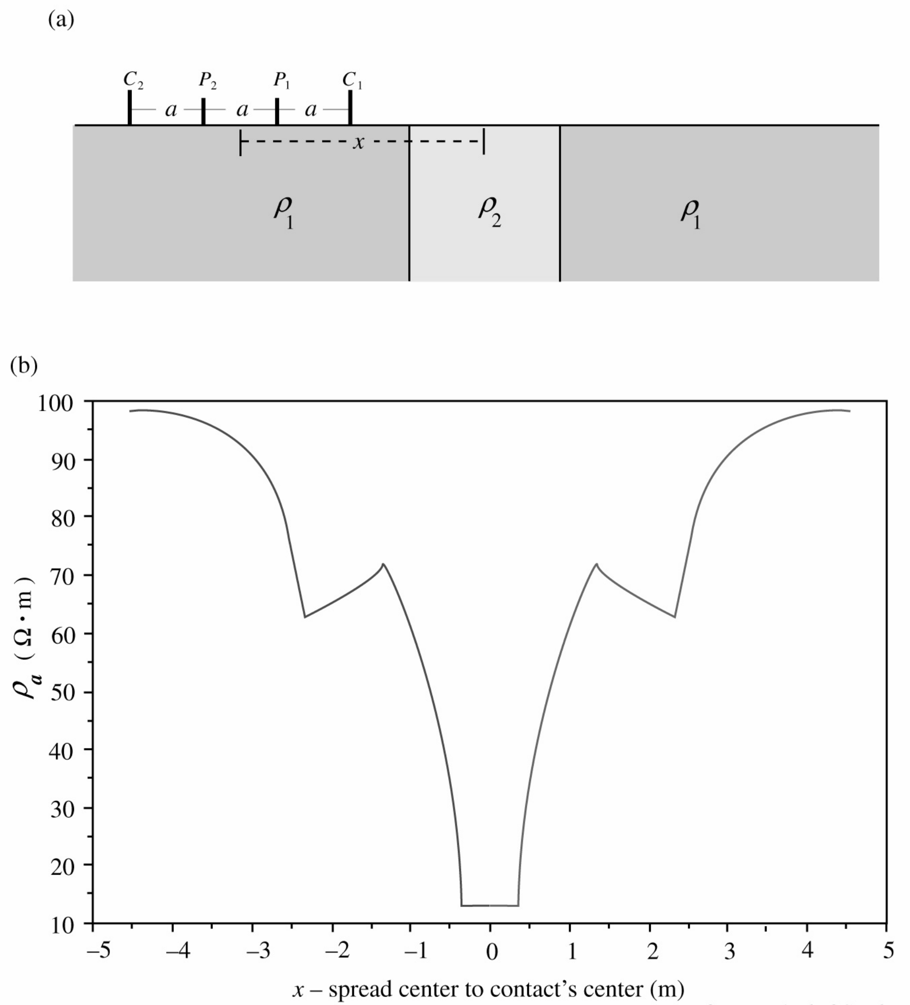

FIGURE 5.25g (b)

Introduction to Applied Geophysics

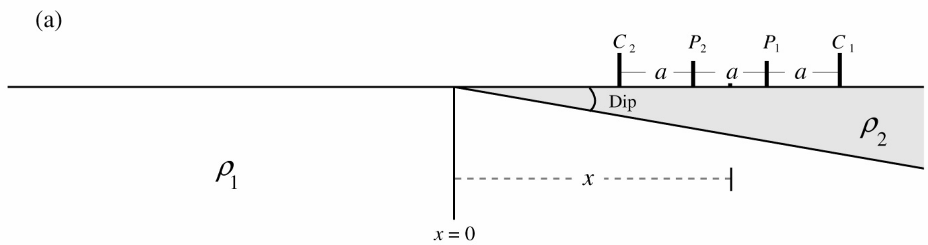

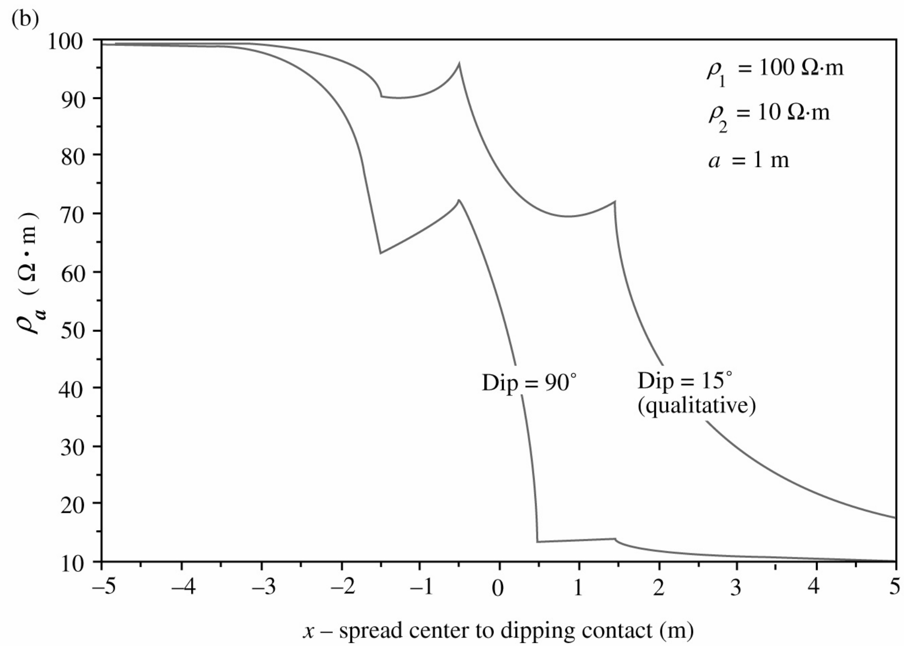

FIGURE 5.27g (b)

Introduction to Applied Geophysics

Resistivity “*Pseudosection*”

- Measurements are a combination of
  profiling (different x) &
  sounding (different a-spacings)
- Plot / contour ρ_{app} versus distance x and a-spacing increment n, where $n = a/a_0$ and a_0 is smallest a-spacing

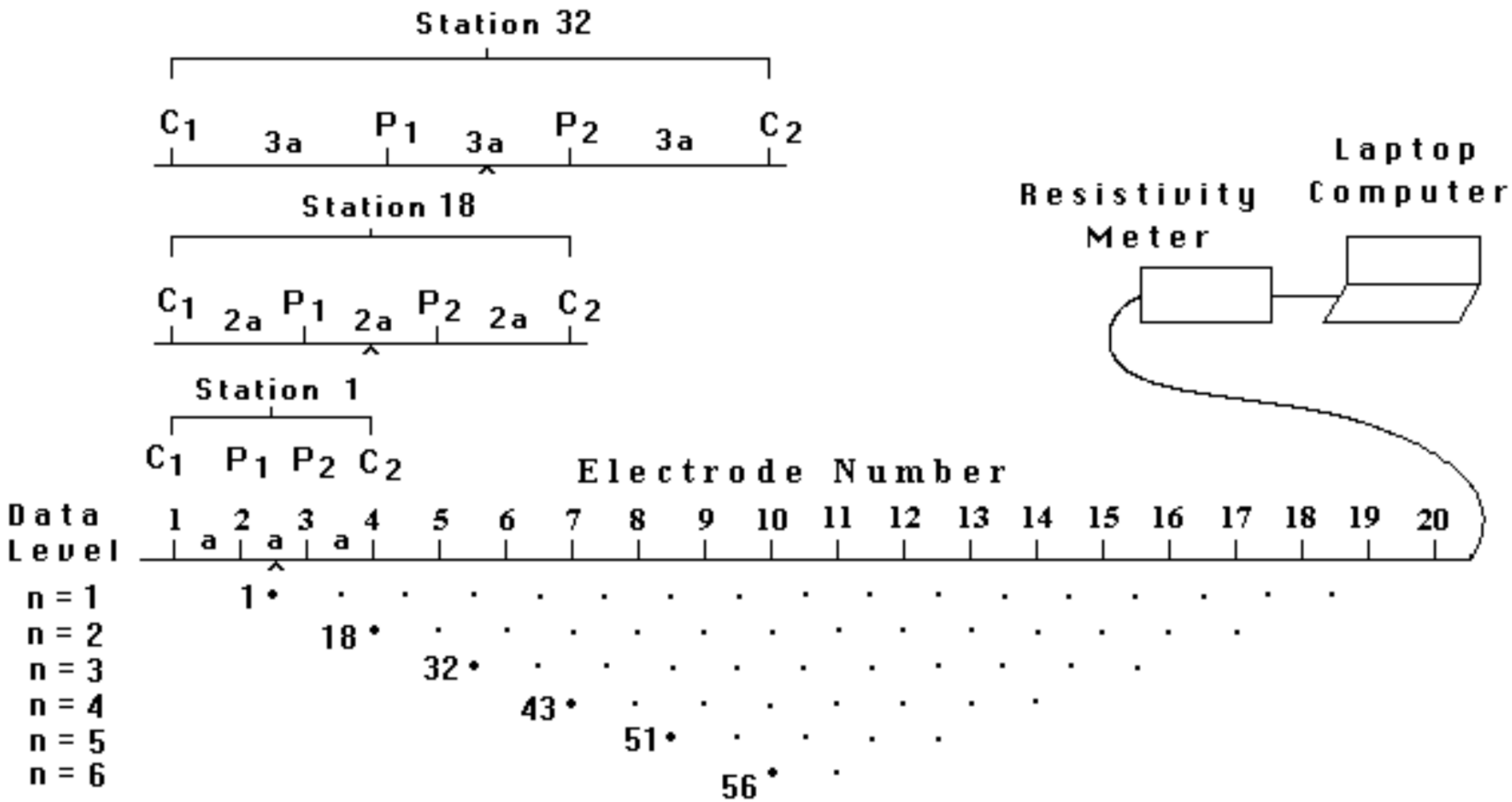

Sequence of measurements to build up a pseudosection

Locke 1999

One technique used to extend horizontally the area covered by the survey, particularly for a system with a limited number of electrodes, is the roll-along method. After completing the sequence of measurements, the cable is moved past one end of the line by several unit electrode spacings. All the measurements which involve the electrodes on part of the cable which do not overlap the original end of the survey line are repeated (Figure 6).

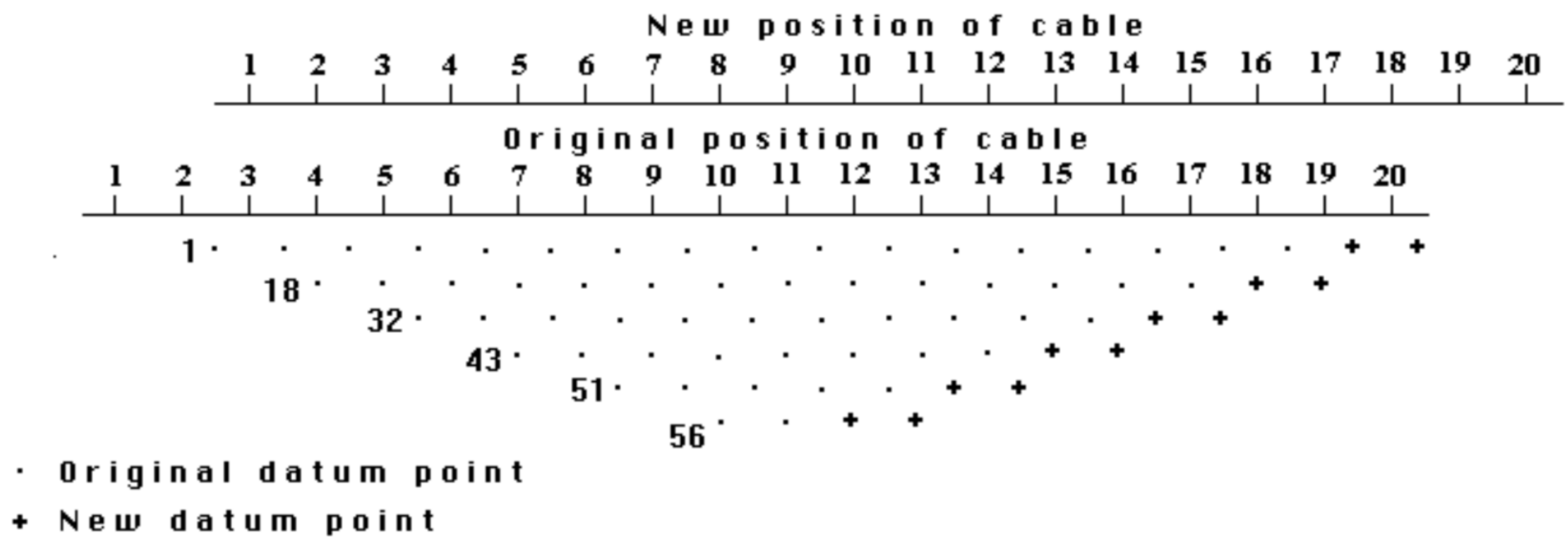

Figure 6. The use of the roll-along method to extend the area covered by a survey.

Locke 1999

(This image from the West Cache fault, collected six years ago, is an example of an apparent resistivity pseudo-section):

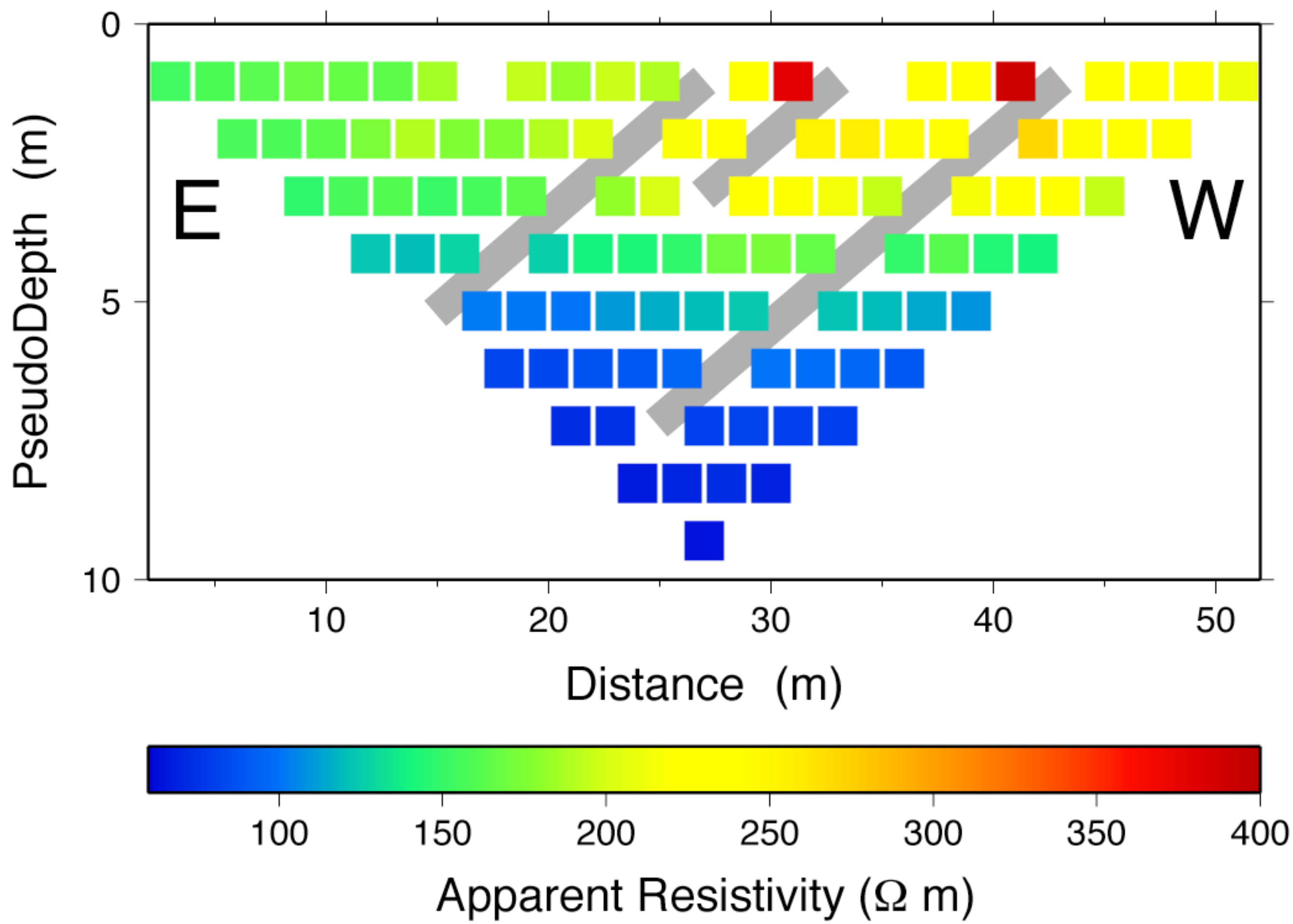

Wenner Array

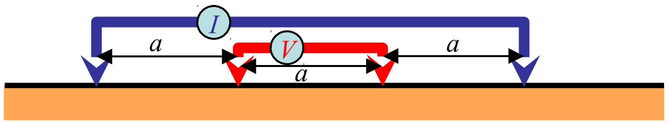

Schlumberger Array

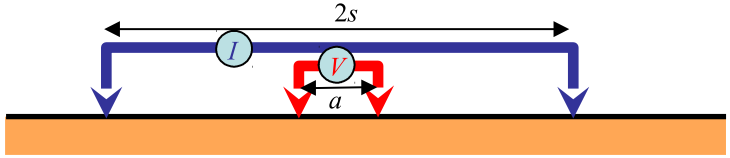

Dipole-Dipole Array

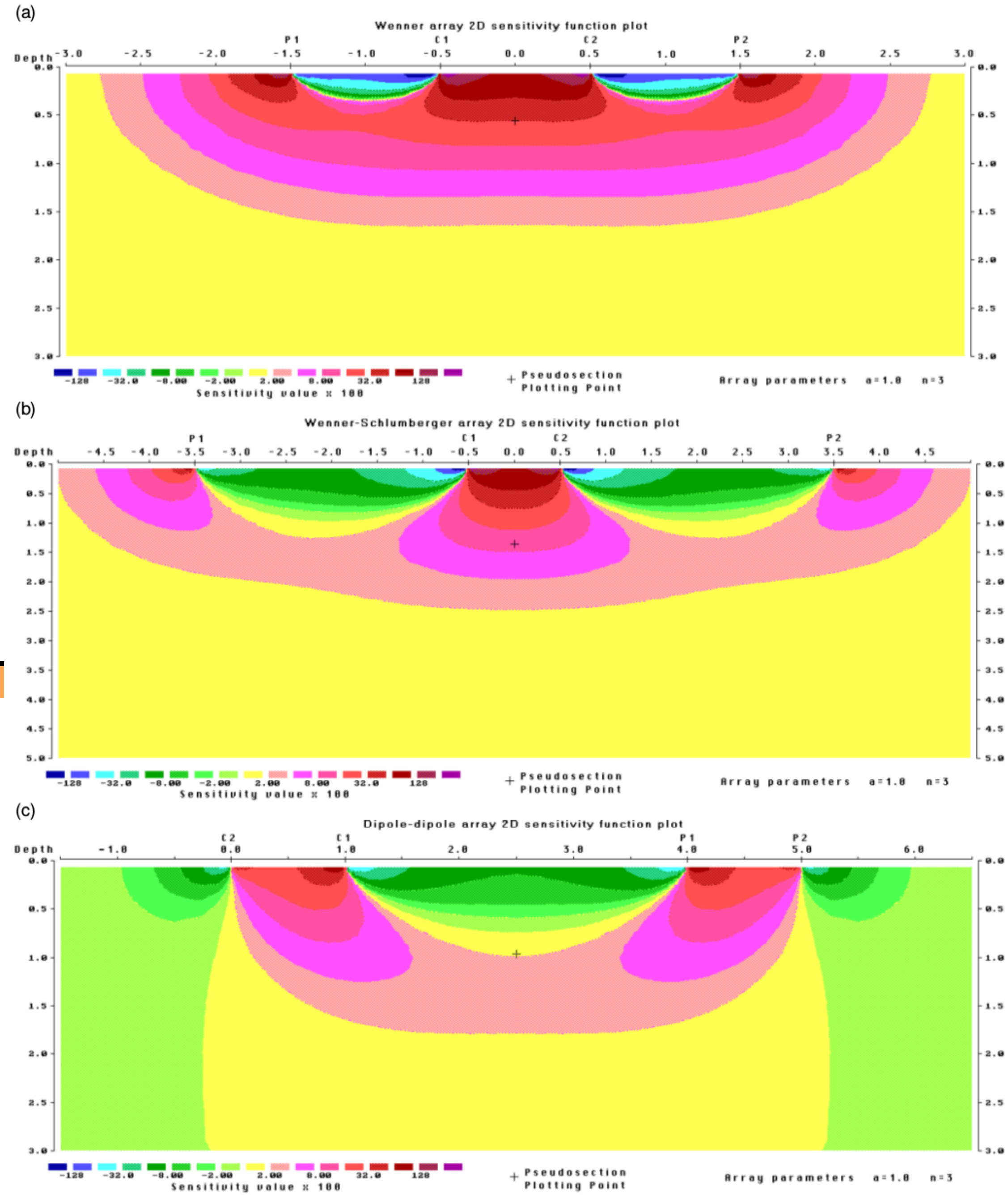

Figure 8. The sensitivity patterns for the (a) Wenner (b) Wenner-Schlumberger and (c) dipole-dipole arrays.

Locke 1999

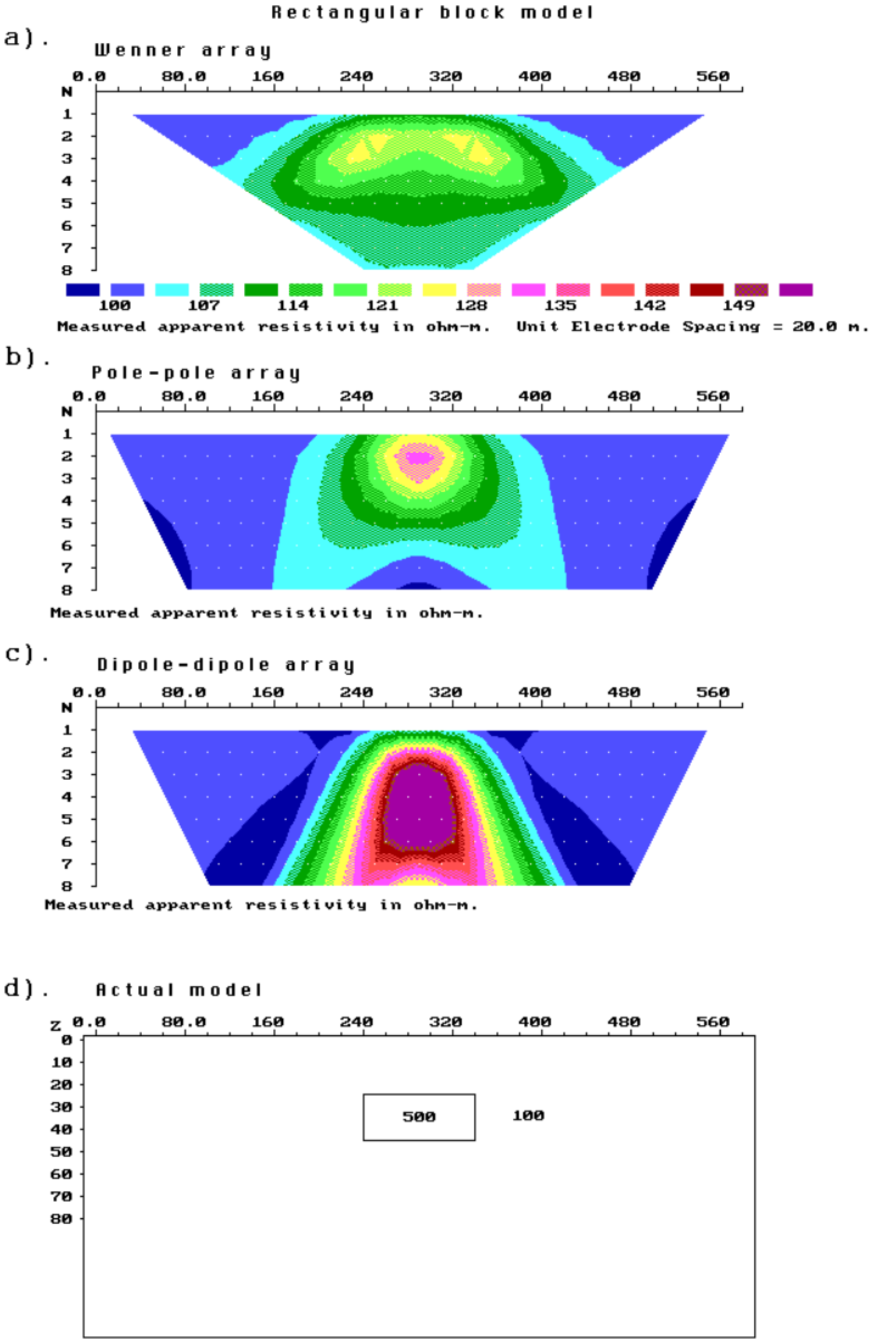

Figure 7. The apparent resistivity pseudosections from 2-D imaging surveys with different arrays over a rectangular block.

Locke 1999

Pseudosection

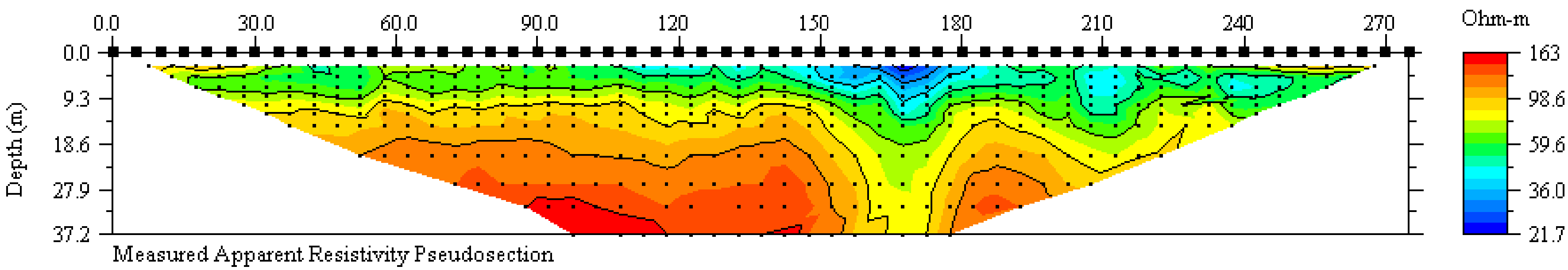

True inversion of the data will yield a much more reliable image (for much the same reasons that depth migration does in the seismic case!)

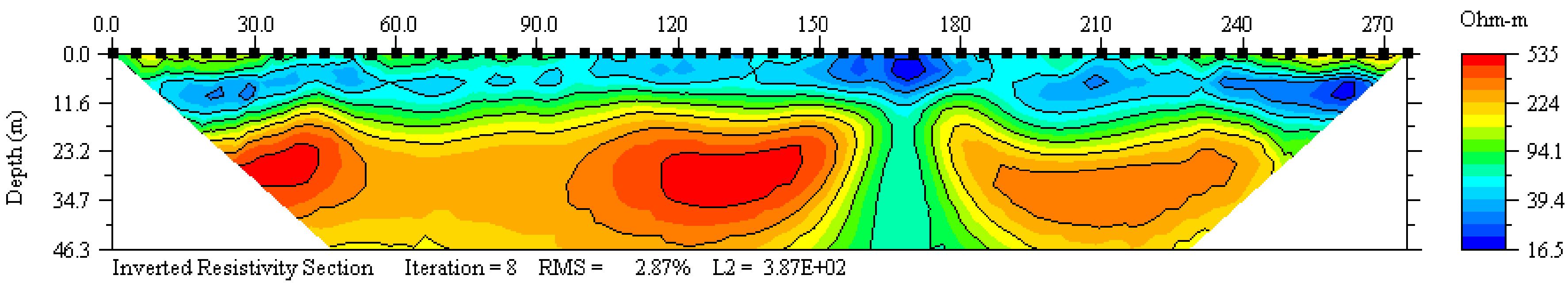

Inversion

East Cache Valley fault zone near Paradise

Resistivity pseudosection from the western trench location

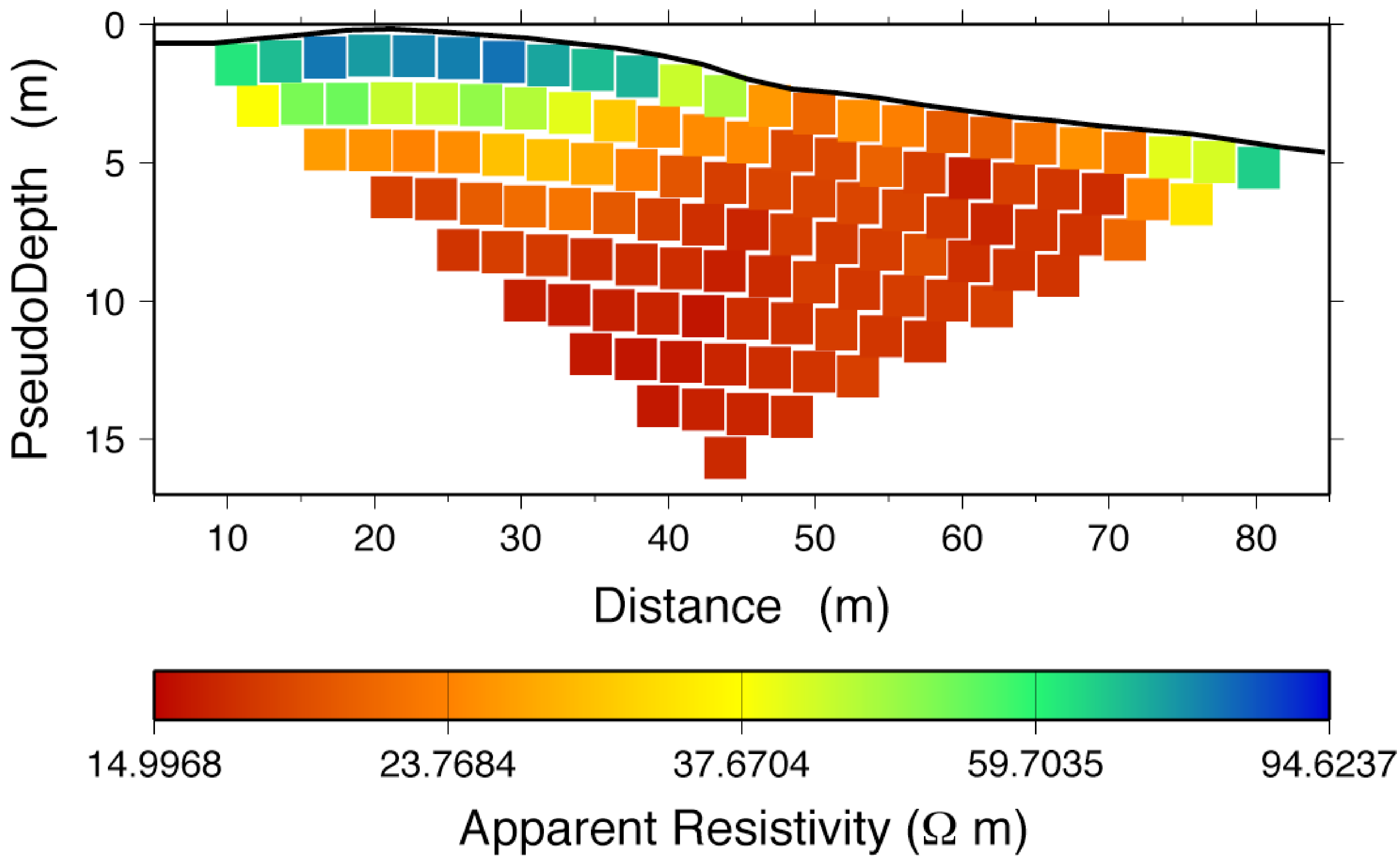

Using resistivity sounding & two layer model:

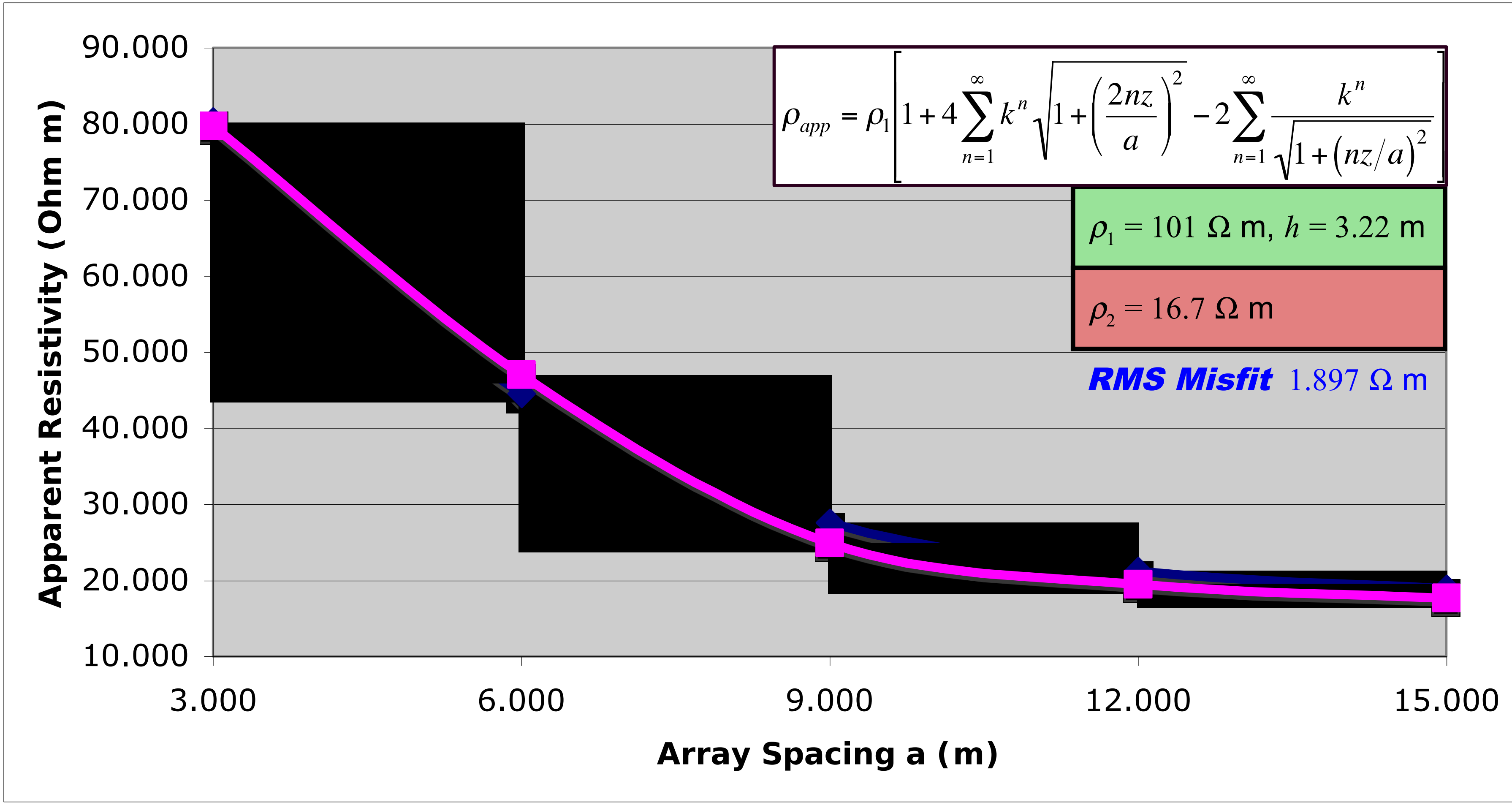

Vertical sounding at 25.7 m. Pink line is measured; Blue line modeled using Excel spreadsheet based on Burger's Table 5-4. Modeling with ***RESIST*** (with interpolated a-spacing) differs in resulting estimates of thickness, but the differences are small.

Can model equally well by using

- constant thickness with varying the resistivities,   OR
- using constant resistivities with varying the thickness !!

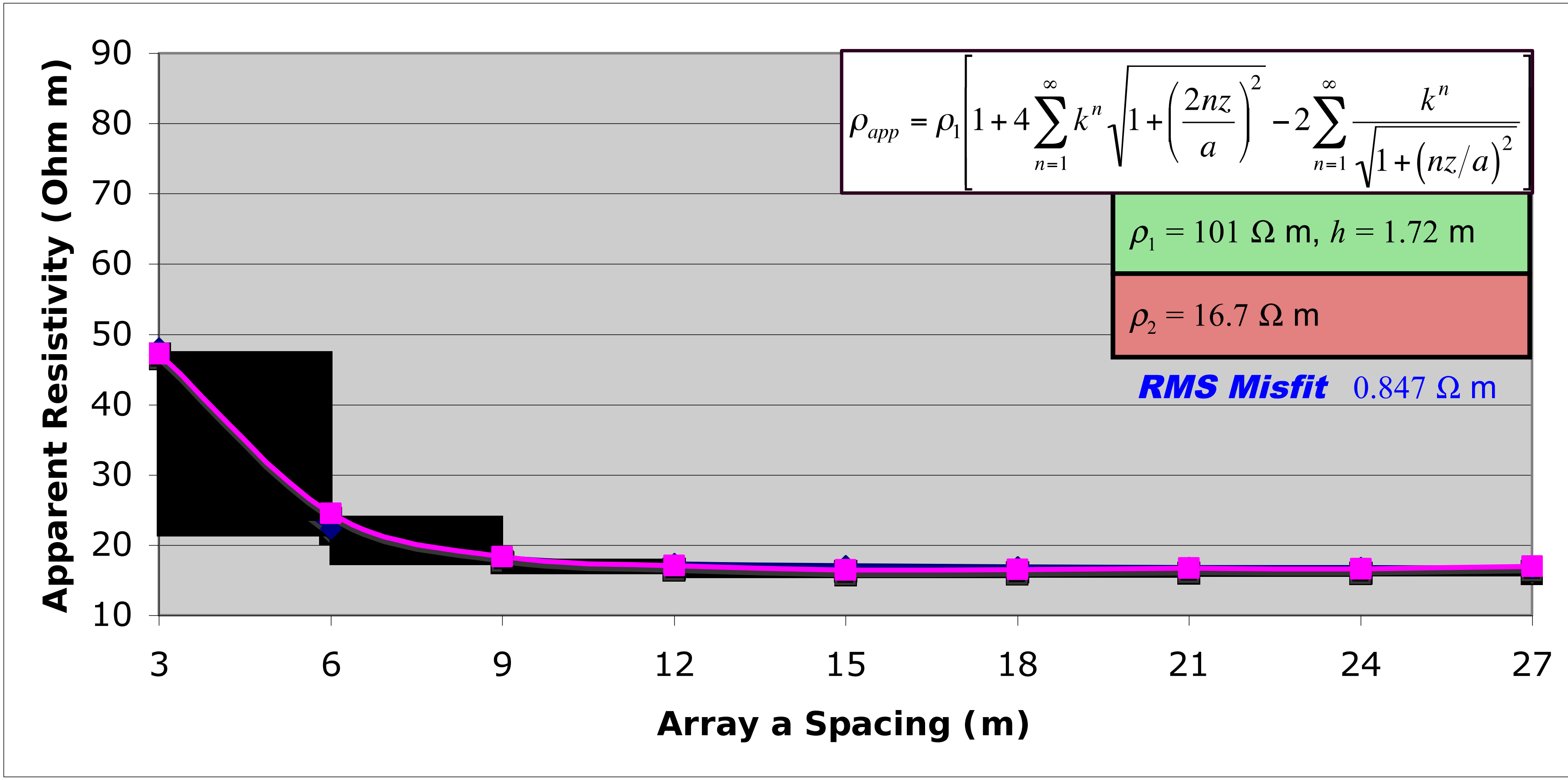

Because these data did not go to a small enough a-spacing to nail down ρ in the upper layer.

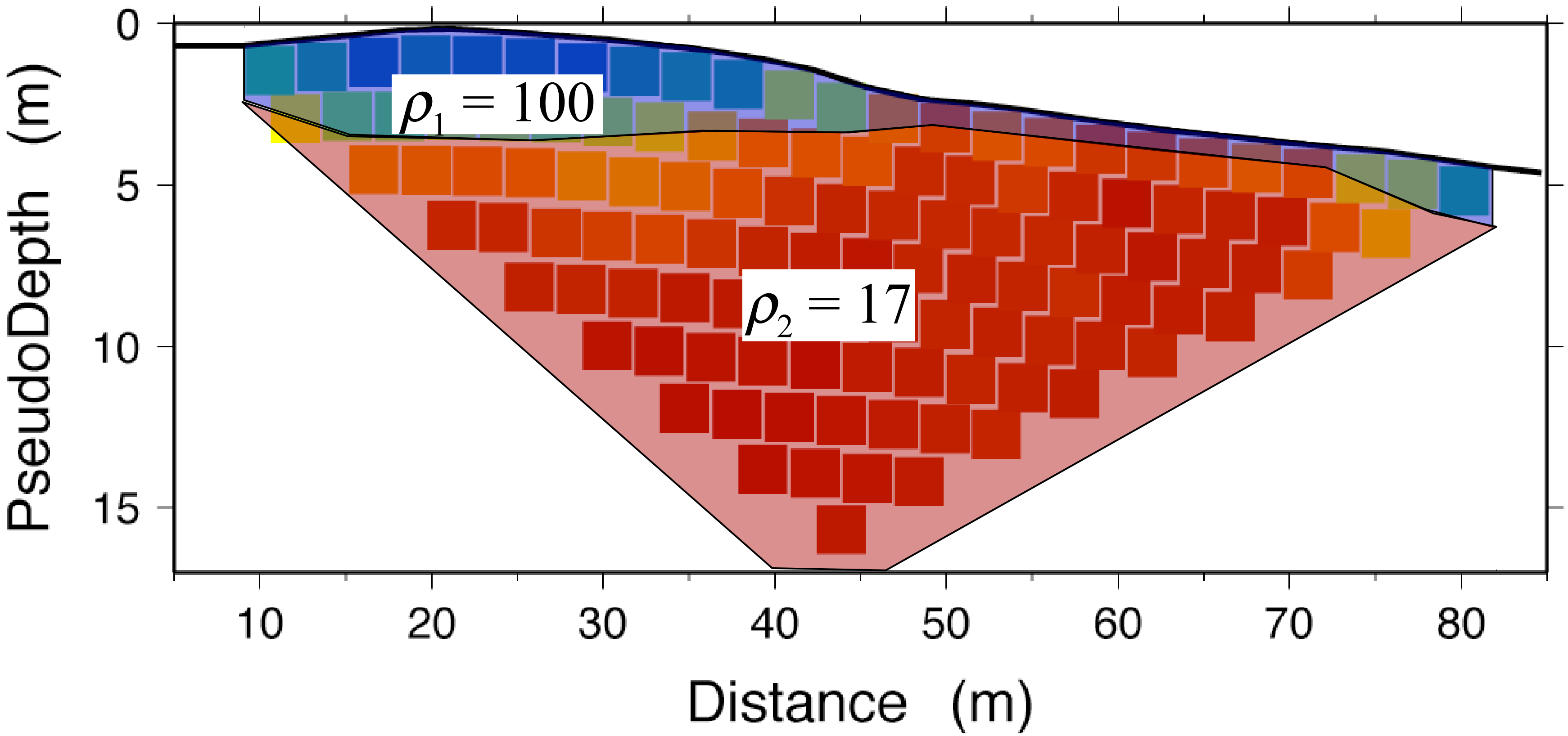

Layer-over-halfspace modeling suggested a variable-thickness upper layer with $\rho \sim 100$ Ω–m (Bonneville deposits) over $\rho = 17$ (Great Salt Lake fm). The data imply the trenched geomorphology represents a beach burm deposit.

East Cache fault in Green Canyon

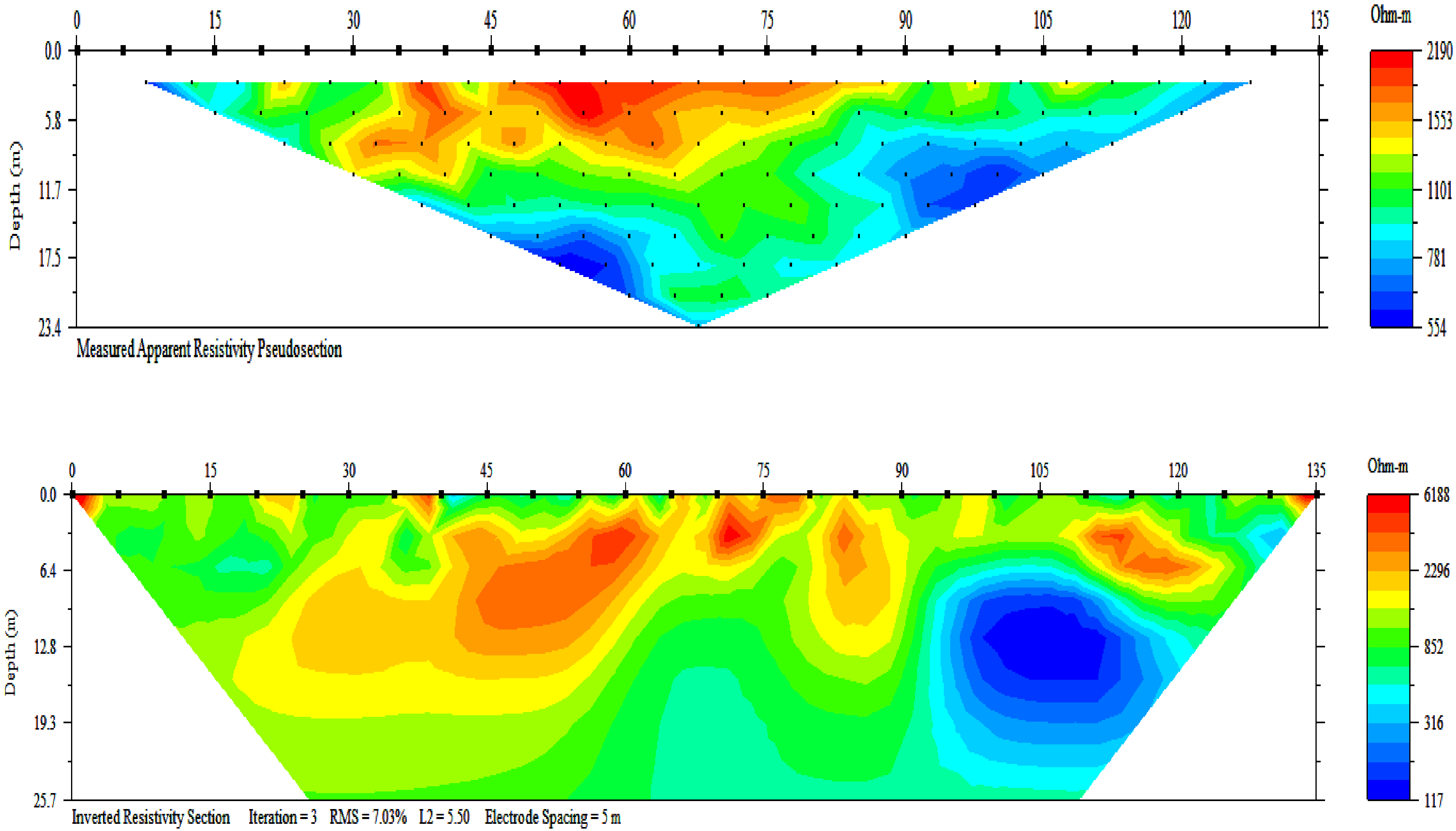

Pseudosection and inversion can be very similar though …

West Cache fault

Apparent resistivity pseudo-section
(collected four years ago)

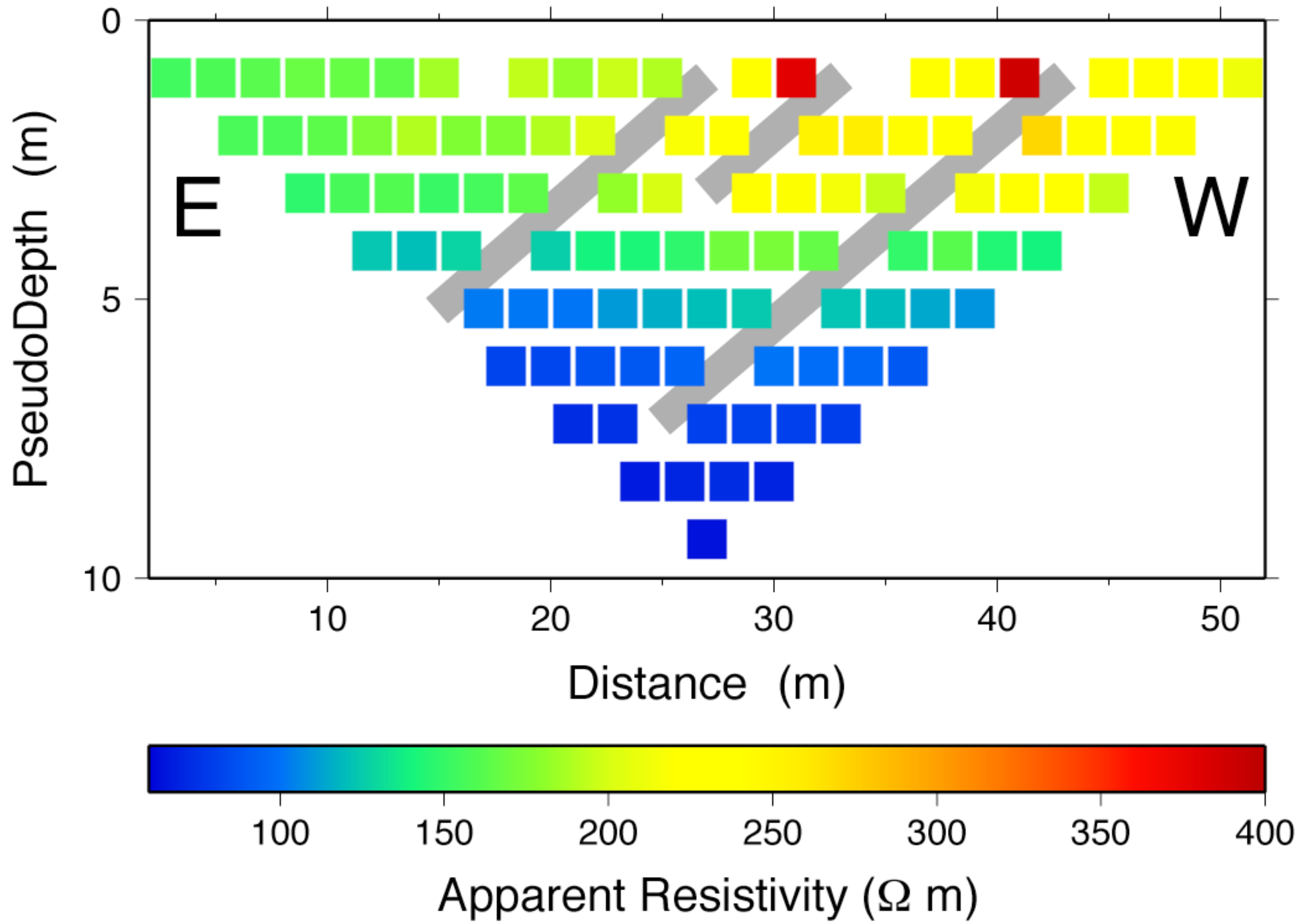

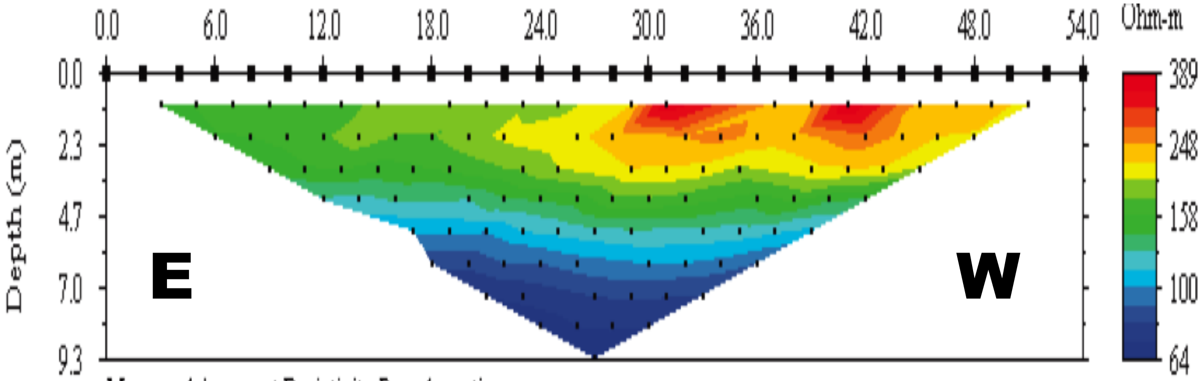

Measured Apparent Resistivity Pseudosection

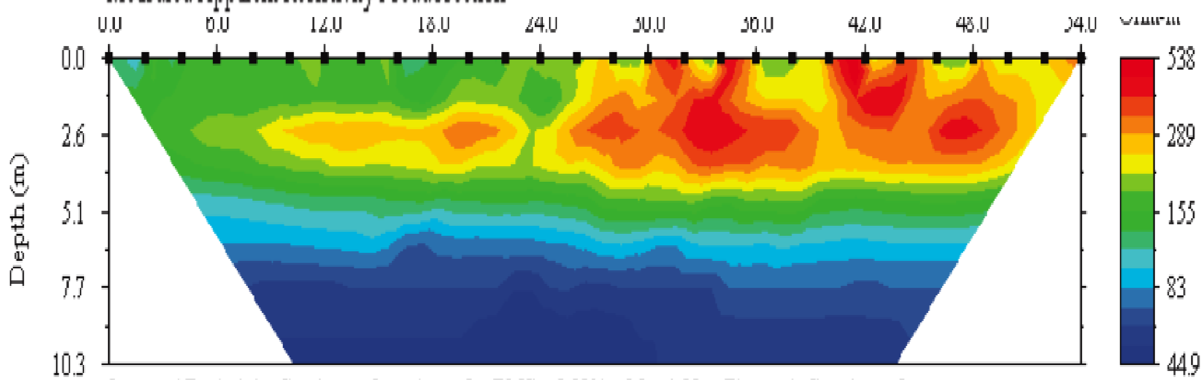

Inverted Resistivity Section Iteration = 2 RMS = 2.99% L2 = 1.00 Electrode Spacing = 2 m

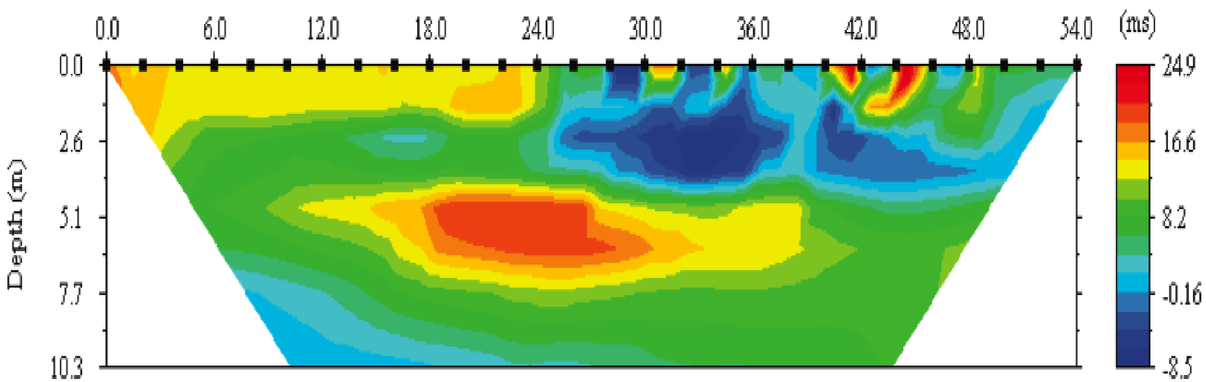

Inverted IP Section Iteration = 1 RMS = 0.89 (ms) Electrode Spacing = 2 m

Measurements at WCF included both DC resistivity and IP (induced potential) ... Here, inverted.

Results plus conditions suggested that the DC resistivity/IP inverted models are not imaging lithology variations but wetting!

Then the west-side high resistivity could be low soil moisture, resulting from retardation of snow-melt in the forested region, while the high-ρ mid-layer on the east side might sit between the water table and a late spring wetting event, rather than a 20-m long (!) wedge of colluvium that is lithologically different from hanging-wall loess. The way to test this possibility would be to repeat the experiment during summer, after the ground has had time to dry out a bit!

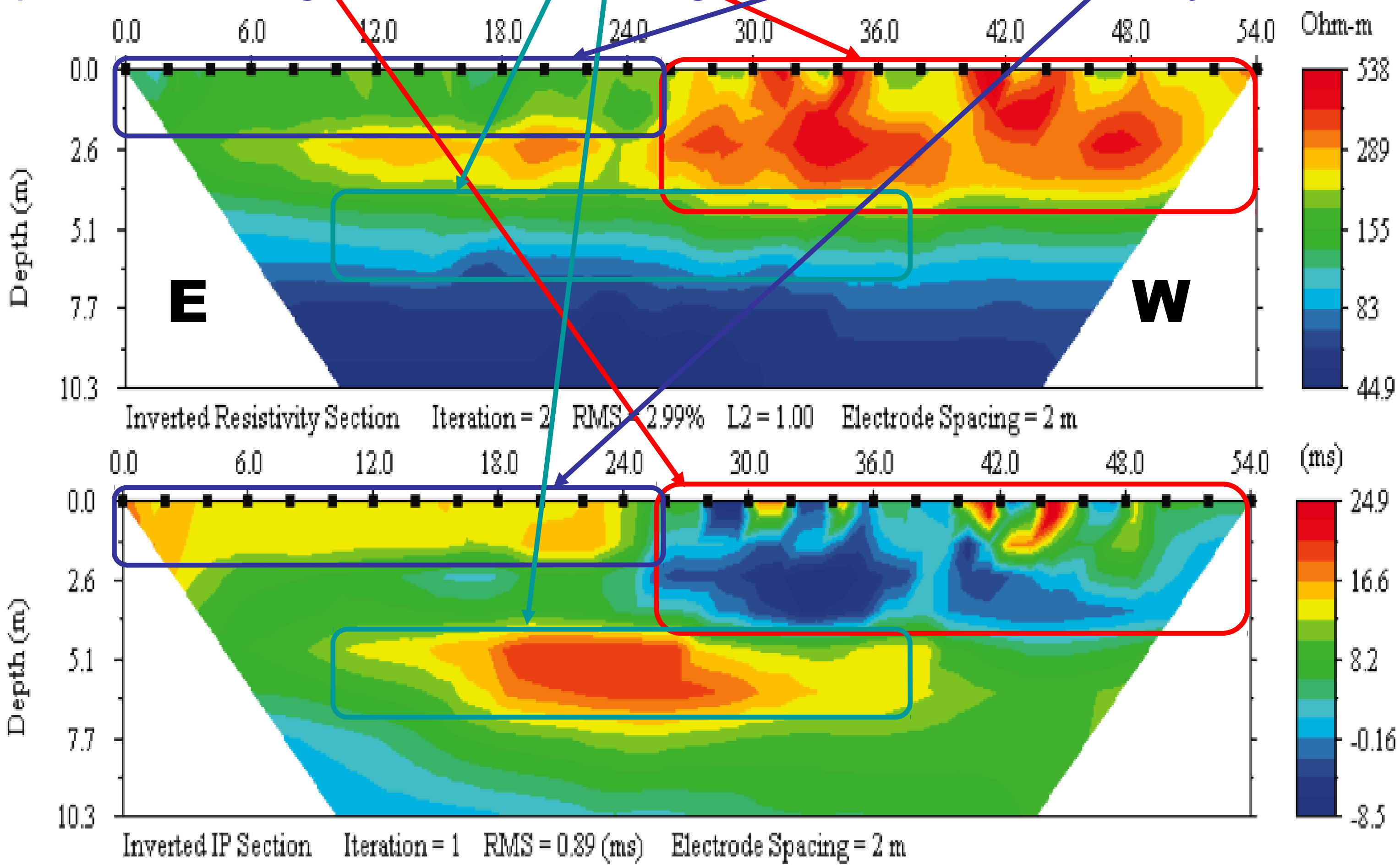

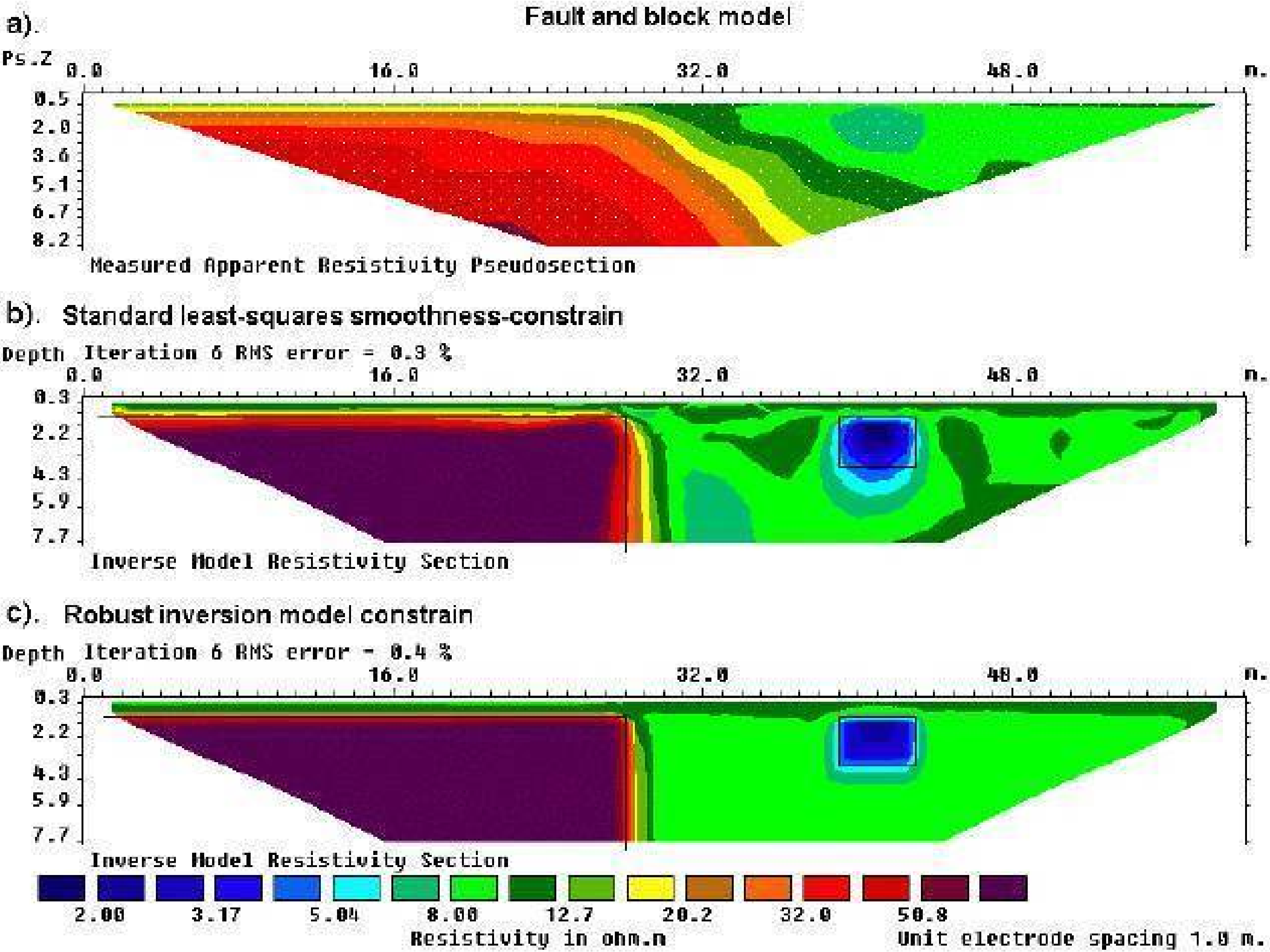
a).
Fault and block model
Ps.Z
0.0
16.0
32.0
48.0
m.
0.5
2.0
3.6
5.1
6.7
8.2
Measured Apparent Resistivity Pseudosection
b).
Standard least-squares smoothness-constrain
Depth Iteration 6 RMS error = 0.3 %
0.0
16.0
32.0
48.0
m.
0.3
2.2
4.3
5.9
7.7
Inverse Model Resistivity Section
c).
Robust inversion model constrain
Depth Iteration 6 RMS error = 0.4 %
0.0
16.0
32.0
48.0
m.
0.3
2.2
4.3
5.9
7.7
Inverse Model Resistivity Section
2.00
3.17
5.04
8.00
12.7
20.2
32.0
50.8
Resistivity in ohm.m
Unit electrode spacing 1.0 m.

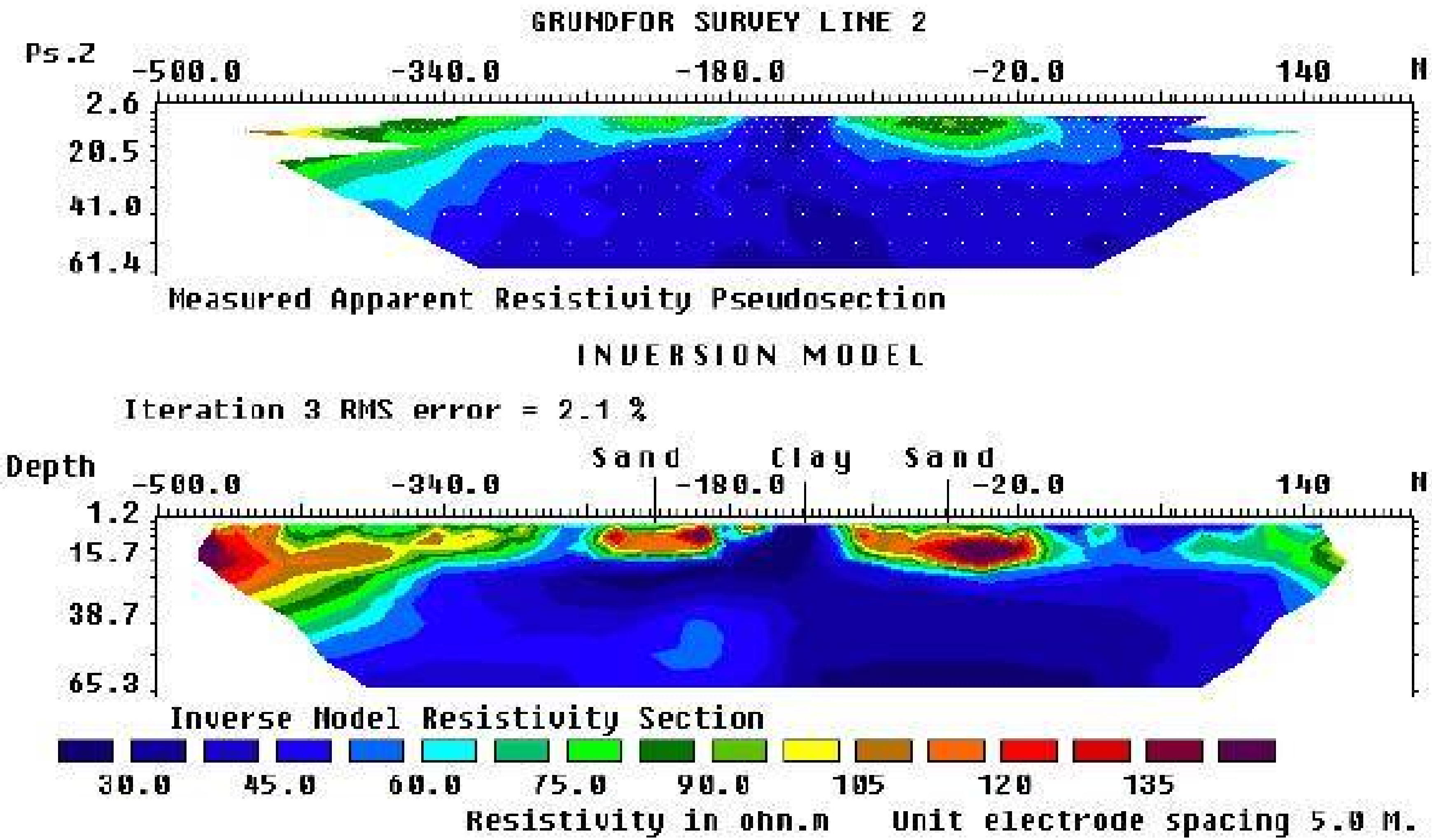

Lithology application: Sand/clay in a study of agricultural groundwater contaminant plumes.

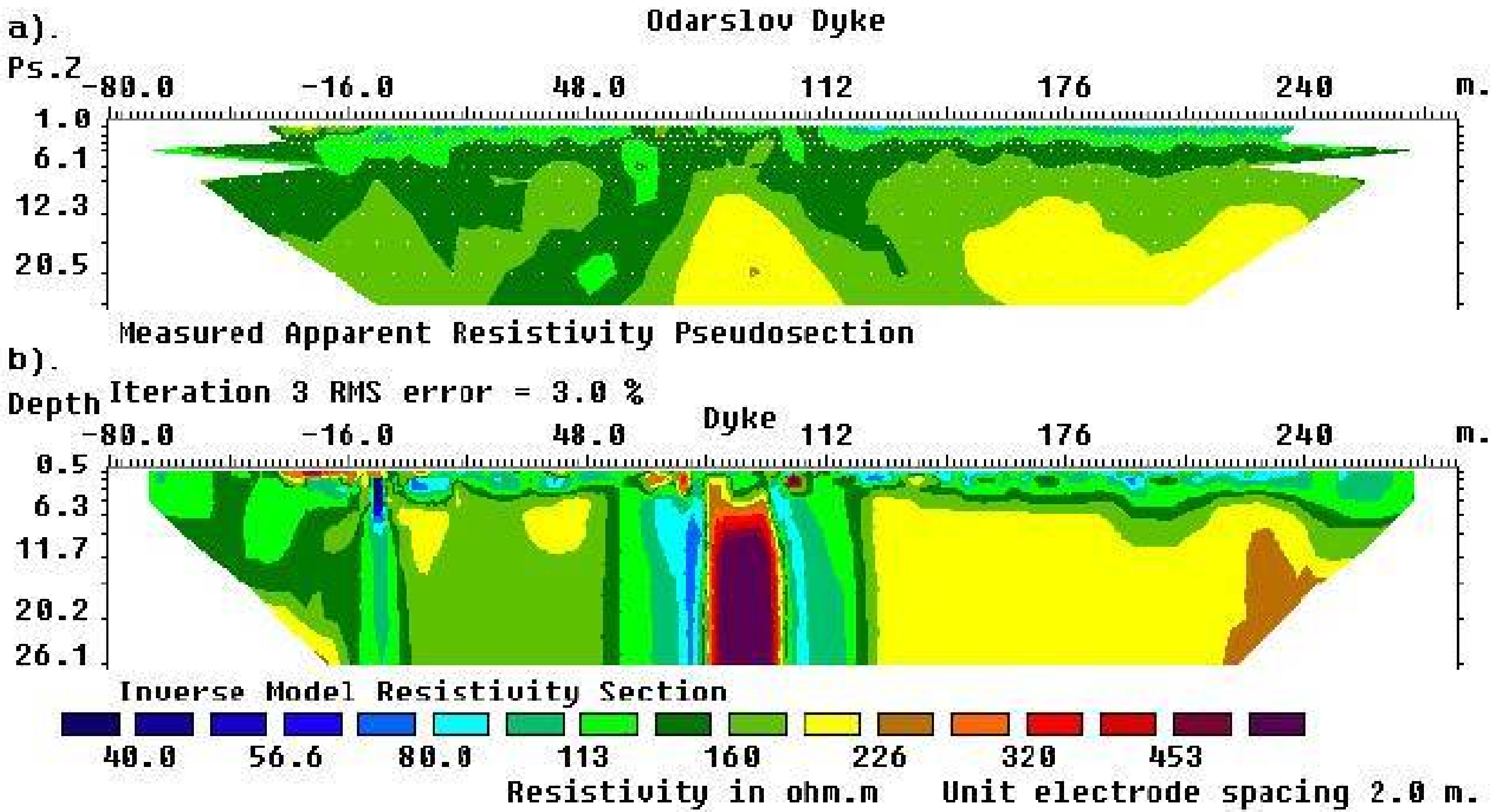

Mapping an intrusive dike feature…

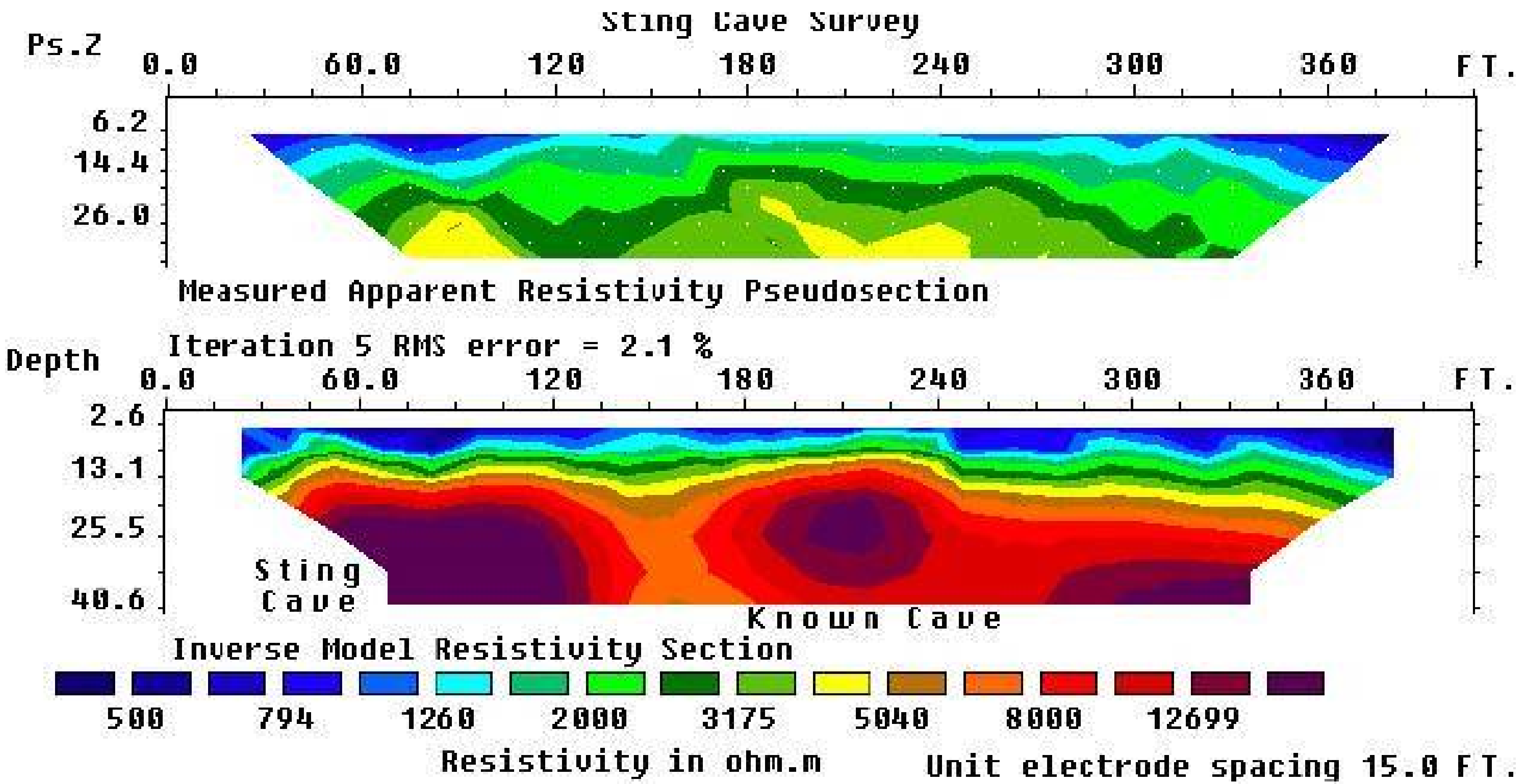

Mapping cave locations in karst terrain.